Journal of Alloys and Compounds 509S (2011) S705–S708

Contents lists available at ScienceDirect

Journal of Alloys and Compounds

journal homepage: www.elsevier.com/locate/jallcom

Nanostructured composites of mesoporous carbons and boranates as hydrogen storage materials

A. Ampoumogli[a], Th. Steriotis[a], P. Trikalitis[b], D. Giasafaki[a,c], E. Gil Bardaji[d], M. Fichtner[d], G. Charalambopoulou[a,*]

[a] National Center for Scientific Research "Demokritos", 15310 Ag. Paraskevi Attikis, Greece
[b] Department of Chemistry, University of Crete, P.O. Box 1470, 71409 Heraklion, Crete, Greece
[c] Department of Materials Science and Engineering, University of Ioannina, 45110 Ioannina, Greece
[d] Institute of Nanotechnology, Karlsruhe Institute of Technology (KIT), Postfach 3640, 76021 Karlsruhe, Germany

ARTICLE INFO

Article history:
Received 11 August 2010
Received in revised form
30 September 2010
Accepted 19 October 2010
Available online 30 October 2010

Keywords:
Hydrogen storage
Complex hydrides
Nanostructured materials
Composite materials
Nanoconfinement
Thermal analysis

ABSTRACT

Nanoconfinement of hydride compounds is receiving considerable attention as an effective method to alleviate the unfavourable thermodynamic properties of complex hydrides hindering their technological application in hydrogen storage. In this work wet-chemistry routes are employed for the incorporation of $NaBH_4$ and $Mg(BH_4)_2$ particles in the porous network of an ordered mesoporous carbon scaffold offering uniform pores with a primary size of 3.5 nm, high surface area and large pore volume. The successful in all cases confinement of the two hydrides leads clearly to a noticeable improvement of their thermal decomposition properties, supporting the direct correlation between particle size and hydrogen delivery performance.

1. Introduction

Complex metal hydrides with high hydrogen content such as boranates (>10 wt% H) are being extensively studied as potential hydrogen storage systems. Nevertheless they still cannot offer technically viable solutions due to their unfavorable kinetic and thermodynamic properties including high thermal stability, slow desorption/absorption kinetics and irreversibility upon cycling resulting from the multi-step reactions and/or formation of by-products during their decomposition [1,2].

Different approaches (formation of hydride mixtures and/or doping with catalysts, high energy or reactive ball milling etc.) have been explored and significant progress has been achieved on tuning the above characteristics, however it has not been yet possible to overcome all limitations and further improvements are necessary. Nanoengineering, targeting to the dramatic decrease of the particle size of hydride materials is currently considered an attractive and promising strategy towards accelerated and enhanced hydrogen discharge/loading, decreased decomposition temperatures and minimised release of by-products. More specifically, it is now well understood that downsizing of hydride phases to the nanoscale leads among others to improved desorption behaviour [3], since such particles in general possess markedly different properties (enhanced surface interactions, faster kinetics, increased number of defects, modified phase transformations) from the respective bulk materials. Metal hydride nanodomains are usually prepared by high-energy ball milling without, however, attaining accurate control of the produced particle sizes [4]. At the same time, mechanically processed hydrides are in a metastable state favouring agglomeration and sintering effects. Quite recently, nanoconfinement, based on the incorporation of hydrides within the pore system of an inert (most commonly carbonaceous) matrix (scaffold), has emerged as a facile pathway to preserve the dimensions of nanosized hydrides and thus modify effectively the dehydrogenation reaction [5]. Several experimental and theoretical studies on such nanoconfined systems have indeed exhibited reduced dehydrogenation temperatures but also improved desorption kinetics [6,7]. Faster dehydrogenation rates, lower hydrogen desorption activation energies/temperatures and increased cycling capacities have in general been obtained from the infiltration of various hydrides such as $NaAlH_4$, MgH_2, $LiBH_4$ and $Mg(BH_4)_2$ in various microporous and mesoporous scaffolds

* Corresponding author. Tel.: +30 210 6503404, fax: +30 210 6525004.
E-mail address: gchar@chem.demokritos.gr (G. Charalambopoulou).

0925-8388/$ – see front matter © 2010 Elsevier B.V. All rights reserved.
doi:10.1016/j.jallcom.2010.10.098

including activated carbon, carbon nanotubes/nanofibers, and carbon aerogels [2,7–10]. These encouraging results have comprised the basis of extensive research focusing on the effect of diverse parameters such as the pore and surface properties of the scaffold, the available gas diffusion paths, the interplay between the porous matrix and the confined hydride, the weight penalties, etc.

In this work we present a facile process for the preparation of hydride–carbon composites based on $NaBH_4$ and $Mg(BH_4)_2$. Taking into account that hydrides infiltration/impregnation is expected to be facilitated by porous scaffolds with controlled pore size but also high surface area and pore volume, we have emphasized on the usage of ordered mesoporous carbons referred to as CMK-3 [11]. This material consists of uniformly sized, interconnected carbon rods arranged in a hexagonal pattern as it is prepared through a nanocasting technique using as template the SBA-15 ordered mesoporous silica. CMK-3 carbons can be considered quite advantageous hydride hosts as: (a) they have a narrow mesopore size distribution centered between 3–5 nm as well as micropores on the mesopores walls, matching the desired size of efficiently dispersed hydride nanoparticles, (b) they exhibit high specific surface areas (>1000 m^2/g) due to micropores and large pore volumes (>1 cm^3/g) due to mesopores, exceeding those offered by the typical carbon scaffolds used so far, (c) they exhibit strong confinement effects (due to micropores) but easy access to the pore system (due to mesopores) and (d) their porosity (i.e. pore size and pore size distribution), morphology and textural properties can be easily tailored by appropriately adjusting the synthesis conditions.

The $NaBH_4$/CMK-3 and $Mg(BH_4)_2$/CMK-3 composites were prepared by a wet impregnation route using liquid NH_3 on the basis of its aprotic nature as well as the high solubility of both hydrides (e.g. 1.04 g/g at 25 °C for $NaBH_4$) [12,13].

2. Materials and methods

2.1. Carbon scaffolds

The CMK-3 ordered mesoporous carbon samples were produced through a standard nanocasting route [14]: a certain amount of the large pore 2-D hexagonal SBA-15 silica (Claytec Inc., USA) was loaded twice with a carbon source (sucrose solution containing sulfuric acid as catalyst), carbonized at 900 °C, and then treated with HF in order to remove the siliceous template and thus enable the formation of a porous carbon with a "negative" replica structure. Prior to use, the as produced CMK-3 carbon was again calcined at 700 °C under Ar for approximately 12 h, in order to remove the surface active groups that could interfere with the nanoconfined hydride.

2.2. Complex hydrides

$NaBH_4$ was purchased from Sigma–Aldrich Co., while $Mg(BH_4)_2$ was synthesised from magnesium hydride and triethylamine borane complex as described elsewhere [15].

2.3. Carbon/hydride nanocomposites

$NaBH_4$ and $Mg(BH_4)_2$ were infiltrated in the pores of the CMK-3 carbon through a wet impregnation route using liquid NH_3. A special Schlenk line was devised to allow the liquefaction of the ammonia in a (double-wall) vessel directly over the reaction flask containing appropriate amounts of the hydrides (25 mg of $NaBH_4$ or 70 mg of $Mg(BH_4)_2$) and the carbon (100 mg). Air and moisture were removed from the system by purging N_2. Subsequently the double-wall vessel was loaded with a dry ice/acetone mixture, the reaction flask was immersed in a dry ice/acetone bath and the N_2 stream was replaced by a mixture of N_2 and NH_3 (99.999%). Anhydrous NH_3 was liquefied upon contact with the cooled inner surface of the double-wall vessel and started to drip into the carbon/hydride containing flask. NH_3 and N_2 were continuously fed in the system until about 50 ml of liquid NH_3 had been accumulated in the reaction container. The system was left overnight under stirring and N_2 flow to remove the ammonia excess. The produced composites were transferred under N_2 atmosphere to glass tubes which were then sealed. Based on the weight of the pure carbon and hydrides used, as well as the total pore volume of the carbon and the bulk densities of the hydrides, loading was roughly estimated around 20% and 40% (pore volume fractions) in the case of the $NaBH_4$ and $Mg(BH_4)_2$ composites, respectively.

2.4. Characterisation

Transmission electron microscope (TEM) images were obtained from a high resolution JEM-2100 instrument equipped with LaB_6 filament and operating at 200 kV using the LowDose procedure provided by the JEOL software, while the samples were continuously handled under inert atmosphere (glove box or flowing dry nitrogen). N_2 isotherms were measured at 77 K on a volumetric gas adsorption analyser (Autosorb-1MP, Quantachrome). Thermal desorption measurements coupled with in-situ mass spectrometry (TPD/MS) were carried out on a home-made experimental setup, comprising of a quartz sample cell (mounted on a furnace that can reach temperatures up to 700 °C) connected through valves with a turbo pump and the inlet capillary of a quadrupole mass spectrometer (OmniStar GSD 301 O1, Pfeiffer). In all cases the samples (after short outgassing under high vacuum at room temperature) were connected to the mass spectrometer and heated to 650 °C with a rate of 3 °C/min while recording the temporal profiles of ion currents (and temperature) for a series of m/z values corresponding to H_2, NH_3, H_2O, B_2H_6 and $(BH)_3(NH)_3$ fragments. Preparation and handling of samples was done in an argon-filled glove box.

3. Results and discussion

The successful synthesis and thus structural order of the CMK-3 scaffold was confirmed both by XRD patterns, depicting strong reflections of a 2-D hexagonal space group, and high resolution TEM images clearly illustrating the expected periodic hexagonal arrangement of the porous matrix. On the other hand, the pore analysis based on N_2 adsorption data at 77 K showed that the various CMK-3 batches produced are characterised by a narrow pore size distribution centered on a mean pore size of approximately 3.5 nm, surface areas of ca. 1500 m^2/g, and total pore volumes of ca. 1.5 cm^3/g.

In an attempt to qualitatively assess the effectiveness of the infiltration process, N_2 porosimetry was employed to investigate the influence of the hydride particles incorporation on the pore properties of the carbon support. The comparison of the N_2 sorption/desorption isotherms (volume sorbed per unit mass, V_s, versus relative pressure, p/p_0) at 77 K measured for all $NaBH_4$/CMK-3 and $Mg(BH_4)_2$/CMK-3 composites against those of the pure carbon support demonstrates a significant reduction of the available surface area and pore volume after the impregnation with the hydride as shown in Fig. 1. It should be mentioned that the comparisons have been made on a carbon mass basis to exclude the reduction of surface areas and pore volumes due to the extra weight of the hydride. It is seen that the shape of the isotherm (and thus qualitatively the pore size distribution) is retained after infiltration, however a significant micropore volume loss is observed, indicating that infiltration occurs mainly in the micropores. In the $NaBH_4$/CMK-3 case illustrated in Fig. 1, the surface area decreased from 1520 to 980 m^2/g, while the total pore volume decreased from 1.49 to 1.15 cm^3/g. It should be mentioned that CMK-3 samples treated with NH_3 but without any hydride (i.e. blank samples) fully retain their surface areas and pore volumes. The notable and consistent change of the respective properties in different samples, as also reported in the literature (e.g. for $LiBH_4$ in a similar scaffold [16], $NaAlH_4$ in commercial porous carbon [17], $Mg(BH_4)_2$ in activated carbon [6], etc.) indicates that in all cases the hydride particles have indeed penetrated the pore network and occupied a large fraction of the void space of the CMK-3 mesoporous carbon. An additional hint of the successful downsizing and confinement of the incorporated hydride grains in the nanoporous structure of the CMK-3 matrix was provided by TEM/EDS studies that were performed for the case of the $Mg(BH_4)_2$/CMK-3 composites (Fig. 2); although no external hydride traces were visible using the transmission electron microscope, whereas the carbon scaffold appeared to preserve its structural integrity after infiltration, EDS analysis consistently revealed clear Mg signals that can only be associated with the pore-confined $Mg(BH_4)_2$ particles.

The thermal properties of the composite systems were studied by thermal desorption-mass spectrometry experiments which

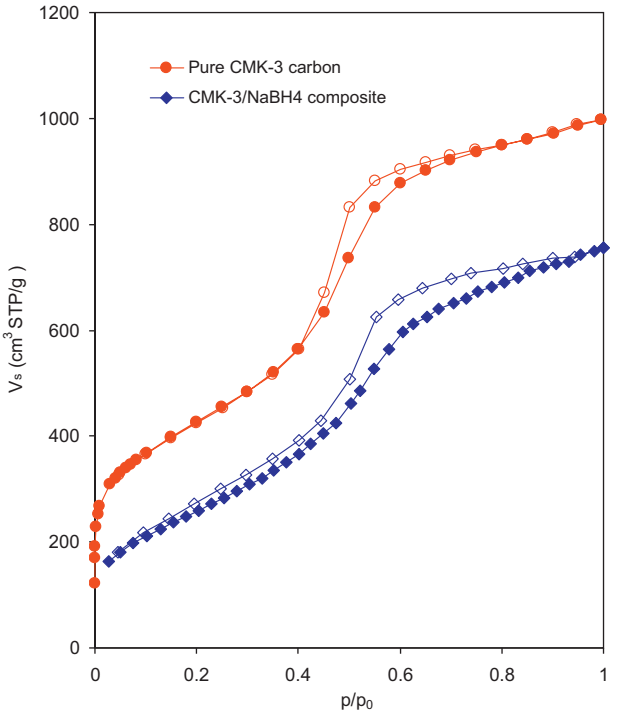

Fig. 1. N_2 sorption desorption isotherms (77 K) on CMK-3 and CMK-3/$NaBH_4$ composite expressed as volume adsorbed per gram of carbon, V_s (closed symbols: adsorption, open symbols: desorption).

demonstrated the direct relation between nanosizing and hydrogen discharging performance. In the case of the 20% $NaBH_4$/CMK-3 sample hydrogen release was seen to commence at a significantly lower temperature compared to the bulk material (Fig. 3). Most interestingly the decomposition profile of the confined hydride exhibits two distinct H_2 peaks at 235 °C and 380 °C, whereas bulk $NaBH_4$ shows practically no activity below approximately 500 °C.

A noticeable shift of the decomposition temperature was also observed in the case of the $Mg(BH_4)_2$/CMK-3 systems. As shown in Fig. 4 the onset of hydrogen gas evolution for the 40% $Mg(BH_4)_2$/CMK-3 sample is around 110 °C, reaching a maximum rate at around 200 °C. The hydrogen profile quenches by the time the sample reaches 350 °C, denoting the temperature at which the first desorption peak of bulk magnesium borohydride is observed. It should be, however, stressed that although hydrogen is the major decomposition product, a considerable quantity of NH_3 is also

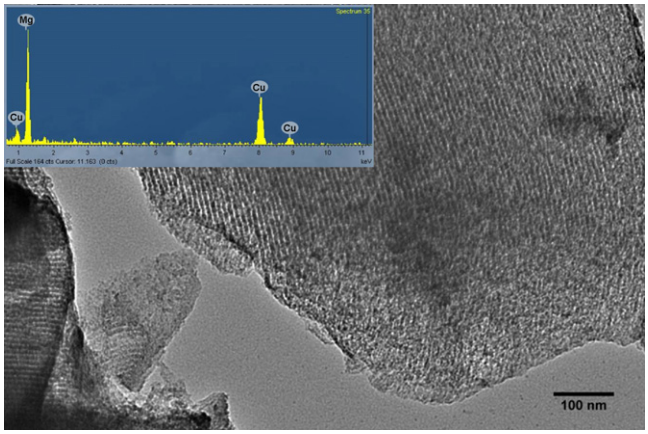

Fig. 2. TEM picture of CMK-3/$Mg(BH_4)_2$ composite. Inset: ED spectrum of the composite (*x*-axis: Energy/keV, *y*-axis: Counts – full scale: 164 counts).

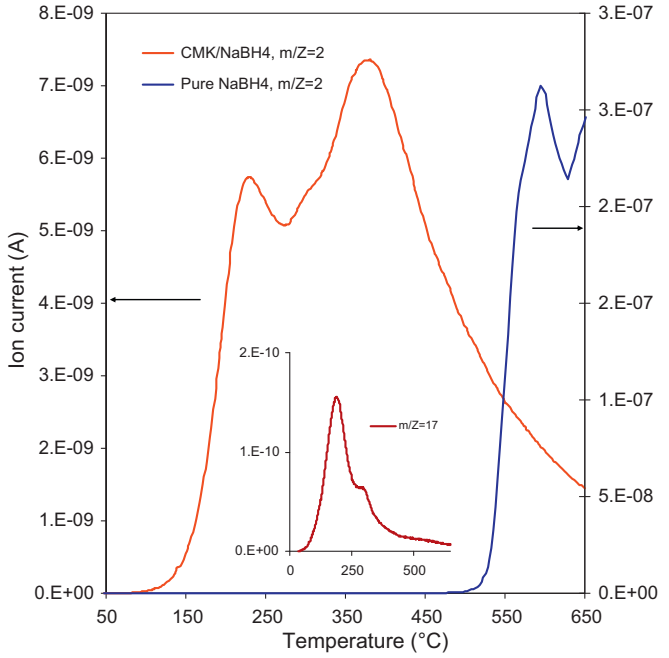

Fig. 3. TDS-MS profiles of hydrogen release from pure $NaBH_4$ and CMK-3/$NaBH_4$ composite (inset: NH_3 release from the composite).

detected (inset of Fig. 4). This is not surprising as based on previous reports $Mg(BH_4)_2$, when treated with ammonia at −70 °C, tends to form the hexaammine complex $Mg(BH_4)_2{\cdot}6NH_3$ [18], the decomposition of which results to the evolution of NH_3 (already at around 80 °C) to afford $Mg(BH_4)_2{\cdot}2NH_3$ (at around 120 °C). The decomposition of the latter is almost complete by 400 °C. On this ground we also performed control TPD/MS measurements on a $Mg(BH_4)_2{\cdot}6NH_3$ (blank) sample, prepared by dissolving solely magnesium borohydride (and omitting the carbon) in liquid ammonia using the procedure described in Section 2.3. The obtained results

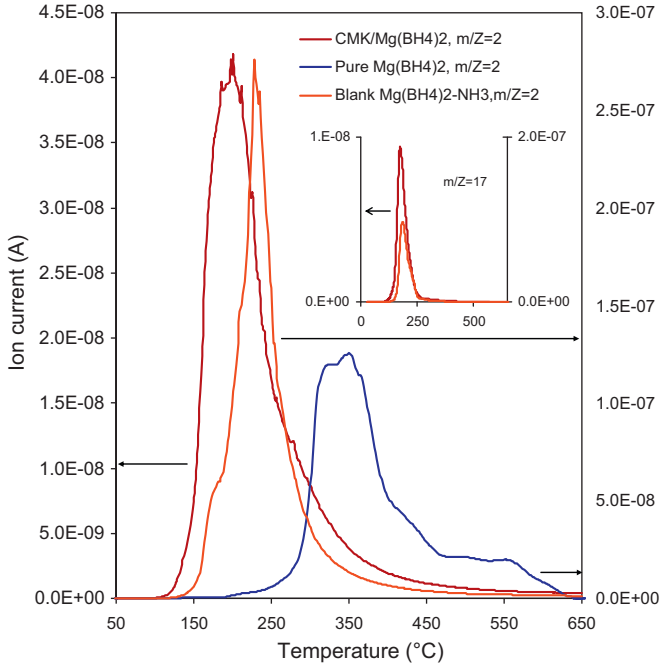

Fig. 4. TDS-MS profiles of hydrogen release from pure $Mg(BH_4)_2$, $Mg(BH_4)_2{\cdot}6NH_3$ complex and CMK-3/$Mg(BH_4)_2$ composite (inset: NH_3 release from the complex and the composite).

(Fig. 4) verify the generation of NH_3 (which most likely also contributes to the signal of the produced H_2) from the non-confined sample and suggest that the NH_3 complex formation destabilises $Mg(BH_4)_2$. The confinement of the NH_3 complex in the CMK-3 pores produces further destabilization leading to decreased decomposition temperature. It should however be mentioned that the reversibility of the system might be questioned and should thus be further explored.

4. Conclusions

The structural and thermal properties of the developed nanocomposites based on the combination of $NaBH_4$ or $Mg(BH_4)_2$ and an ordered mesoporous carbon matrix support the positive effect that nanosizing can have on the decomposition behaviour of the bulk hydride. The adopted synthesis protocols based on the dissolution of the hydrides in liquid ammonia enabled the nanoconfinement and the improvement of thermal properties of the hydrides particles, nevertheless further work is clearly necessary to address a number of issues such as the cyclability and reversibility of the system as well as the effect of ammonia complex formation and consequent ammonia release during the first decomposition cycle.

Acknowledgements

Partial funding by the EU project NANOHY (FP7 Grant Agreement 210092) is gratefully acknowledged.

References

[1] S. Satyapal, J. Petrovic, C. Read, G. Thomas, G. Ordaz, Catalysis Today 120 (2007) 246–256.
[2] J.J. Vajo, G.L. Olson, Scr. Mater. 56 (2007) 829–834.
[3] M. Ficthner, Nanotechnology 20 (2009) 204009.
[4] H.W. Brinks, B.C. Hauback, S.S. Srinivasan, C.M. Jensen, J. Phys. Chem. B 109 (2005) 15780–15785.
[5] H. Wu, Chem. Phys. Chem. 9 (2008) 2157–2162.
[6] M. Fichtner, Z. Zhao-Karger, J. Hu, A. Roth, P. Weidler, Nanotechnology 20 (2009) 204029.
[7] S. Zhang, A.F. Gross, S.L. Van Atta, M. Lopez, P. Liu, C.C. Ahn, J.J. Vajo, C.M. Jensen, Nanotechnology 20 (2009) 204027.
[8] F. Schüth, B. Bogdanovic, M. Felderhoff, Chem. Commun. (2004) 2249–2258.
[9] C.P. Baldé, B.P.C. Hereijgers, J.H. Bitter, K.P. de Jong, Angew. Chem. Int. Ed. 45 (2006) 3501–3503.
[10] A.F. Gross, J.J. Vajo, S.L. Van Atta, G.L. Olson, J. Phys. Chem. C 112 (2008) 5651–5657.
[11] R. Ryoo, S.H. Joo, M. Kruk, M. Jaroniec, Adv. Mater. 13 (2001) 677–681.
[12] R.C. Wade, United States Patent 4404122 (1983).
[13] H.C. Brown, E.J. Mead, B.C. Subba Rao, J. Am. Chem. Soc. 77 (1955) 6209–6213.
[14] S. Jun, S.H. Joo, R. Ryoo, M. Kruk, M. Jaroniec, Z. Liu, T. Ohsuna, O. Terasaki, J. Am. Chem. Soc. 122 (2000) 10712–10713.
[15] K. Chlopek, Ch. Frommen, A. Léon, O. Zabara, M. Fichtner, J. Mater. Chem. 17 (2007) 3496–3503.
[16] X. Liu, D. Peaslee, C.Z. Jost, E.H. Majzoub, J. Phys. Chem. C 114 (2010) 14036–14041.
[17] J. Gao, Ph. Adelhelm, M.H.W. Verkuijlen, C. Rongeat, M. Herrich, P.J.M. van Bentum, O. Gutfleisch, A.P.M. Kentgens, K.P. de Jong, P.E. de Jongh, J. Phys. Chem. C 114 (2010) 4675–4682.
[18] G. Soloveichik, J.H. Her, P.W. Stephens, Y. Gao, J. Rijssenbeek, M. Andrus, J.-C. Zhao, Inorg. Chem. 47 (2008) 4290–4298.